Lowest excited triplet state of 2,5-dimethyl-1,3,5-hexatriene: Resonance Raman spectra and quantum chemical calculations

ARTICLE *in* THE JOURNAL OF PHYSICAL CHEMISTRY · SEPTEMBER 1991

Impact Factor: 2.78 · DOI: 10.1021/j100171a029

6 AUTHORS, INCLUDING:

Fabrizia Negri
University of Bologna
160 PUBLICATIONS **3,967** CITATIONS
SEE PROFILE

Albert M Brouwer
University of Amsterdam
142 PUBLICATIONS **3,423** CITATIONS
SEE PROFILE

Søren Møller
Roskilde University
30 PUBLICATIONS **463** CITATIONS
SEE PROFILE

Lowest Excited Triplet State of 2,5-Dimethyl-1,3,5-hexatriene: Resonance Raman Spectra and Quantum Chemical Calculations

Fabrizia Negri, Giorgio Orlandi,*

Dipartimento di Chimica "G.Ciamician", University of Bologna, I-40126 Bologna, Italy

Albert M. Brouwer,

Laboratory of Organic Chemistry, University of Amsterdam, Nieuwe Achtergracht 129, NL-1018 WS Amsterdam, The Netherlands

Frans W. Langkilde,

Department of Physical Chemistry A, Royal Danish School of Pharmacy, 2 Universitetsparken, DK-2100 Copenhagen, Denmark

Søren Møller, and Robert Wilbrandt*

Department of Environmental Science and Technology, Risø National Laboratory, DK-4000 Roskilde, Denmark *(Received: December 28, 1990)*

Theoretical and Raman spectroscopic studies are presented of the ground and lowest excited triplet states of (*E*)- and (*Z*)-2,5-dimethyl-1,3,5-hexatriene and their 3,4-dideuterio and 3-deuterio isotopomers. The T_1 potential energy surface is calculated from SCF-LCAO-MO-CI theory. Energy minima and equilibrium geometries are determined in the T_1 state. Frequencies and normal modes of vibrations are calculated for the minima of the T_1 and S_0 states. Energies of higher triplet levels are computed and oscillator strengths for the $T_1 \rightarrow T_n$ transitions are determined. The displacements in equilibrium geometries between the T_1 and the T_n level corresponding to the strongest $T_1 \rightarrow T_n$ transition are calculated and are used to estimate the intensities of the resonance Raman spectra of the T_1 state under the assumption of a predominant Franck-Condon scattering mechanism. The influence of the ground-state conformation around C-C single bonds on T_1 resonance Raman spectra is considered in detail for the two isomers. It is found that for the *E* isomers the *tEt* and for the *Z* isomers the *tEc* forms are the predominant ones in the T_1 state. The *Z* forms are at considerable higher energy than the *E* forms in the T_1 state due to nonbonded interaction. A good agreement is found between theoretically calculated and experimental spectra. The results are compared with previously published data for 1,3,5-hexatriene.

Introduction

In previous studies[1-3] we considered the transient resonance Raman (TRR) spectra of 1,3,5-hexatriene (HT) in its T_1 state with the purpose of obtaining information about the geometry of the T_1 intermediate and about the mechanism of the cis-trans photoisomerization in T_1. The experimental TRR spectra, which have been found to be identical in experiments on solutions of either of the two ground-state isomers, were interpreted by quantum mechanical calculations of equilibrium geometries and vibrational frequencies at the trans (*E*), cis (*Z*), and centrally twisted (*P*) geometries in T_1 and in the T_n state responsible for the TRR activity. On the basis of these calculations the T_1 normal modes showing the strongest Franck-Condon activity in the TRR spectra could be identified for each geometric isomer of HT. The observed TRR spectra were shown to result from a superposition of the spectra of the *Z* and *E* forms with possible weak contributions from the *P* form. It was concluded that the transient T_1 intermediate in the photoisomerization of HT, monitored by TRR spectra, exists as an equilibrium between several geometric structures, in which planar molecules represent a substantial fraction, and that a possible minimum of the potential energy curve at the centrally twisted geometry must be rather shallow.

In this paper we consider the TRR spectra of the T_1 intermediate of the 2,5-dimethyl derivative of HT, 2,5-dimethyl-1,3,5-hexatriene (DMHT). Due to the presence of two CH_3 groups and to the steric strain associated with them, we may expect modifications of the electronic potential energy surfaces (PES) compared with HT. In particular, the potential energy curve for cis-trans photoisomerization of DMHT could be different from for HT. In addition, the different trans-cis (*t-c*) conformers with respect to the two CC single bonds could be roughly isoenergetic in DMHT, due to similar nonbonded interactions of CH_3 and $=CH_2$ groups, and this may lead to the presence of several additional species that need to be considered in the calculations. Experimentally, it has been found for the ground state that the *E* form corresponds to only one conformer, namely *tEt*, while the *Z* form is associated predominantly with the *tZc* conformer with a minor fraction of the *cZc* conformer.[4] Figure 1 shows a planar representation of the six possible ground-state geometries of DMHT. In reality, some of the forms are nonplanar.

The T_1 TRR spectra of the two isomers of nondeuteriated DMHT have been reported previously.[5] The spectra of (*E*)- and (*Z*)-DMHT-*3,4-d*$_2$ and of (*E*)-DMHT-*3-d* are reported in the present paper together with remeasured spectra of DMHT-d_0. The experimental TRR spectra of (*E*)- and (*Z*)-2,5-DMHT have been found to be different.[5] This is reasonable since in T_1 the CC "single" bonds become shorter, and consequently, the barrier for rotation becomes too high for the molecule to be able to interconvert among the different conformers during the T_1 lifetime (~80-170 ns[5]). In other words, the principle of nonequilibration of excited rotamers (NEER) previously formulated for excited singlet states[6,7] is valid also for the longer lived T_1 states of DMHT.

(1) Langkilde, F. W.; Jensen, N. H.; Wilbrandt, R. *J. Phys. Chem.* **1987**, *91*, 1040.
(2) Negri, F.; Orlandi, G.; Brouwer, A. M.; Langkilde, F. W.; Wilbrandt, R. *J. Chem. Phys.* **1989**, *90*, 5944.
(3) Langkilde, F. W.; Wilbrandt, R.; Møller, S.; Brouwer, A. M.; Negri, F.; Orlandi, G. *J. Phys. Chem.*, previous paper in this issue.
(4) (a) Brouwer, A. M. Ph.D. Thesis, University of Leiden, 1987. (b) Brouwer, A. M.; Cornelisse, J.; Jacobs, H. J. C. *Tetrahedron* **1987**, *43*, 435.
(5) Langkilde, F. W.; Jensen, N. H.; Wilbrandt, R.; Brouwer, A. M.; Jacobs, H. J. C. *J. Phys. Chem.* **1987**, *91*, 1029.

0022-3654/91/2095-6895$02.50/0

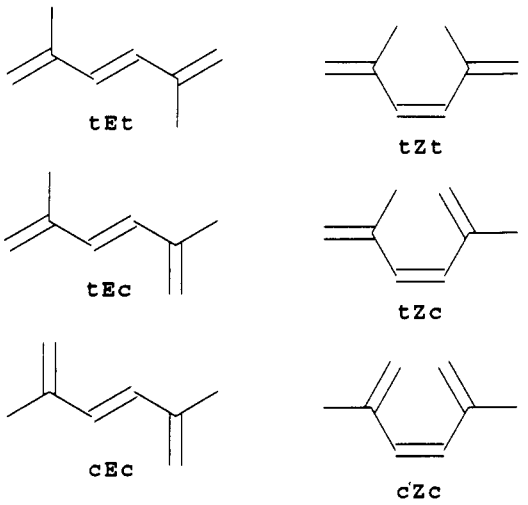

Figure 1. Planar ground-state forms of DMHT.

At the same time, the DMHT molecules are able to equilibrate freely among the *E*, *Z*, and *P* forms, obtained by rotation around the central C=C bond, as the barrier for this interconversion, if any, is expected to be low. Hence, the TRR spectra obtained from (*E*)-2,5-DMHT or (*Z*)-2,5-DMHT in T_1 are expected to be due to a superposition of the spectra of *E*, *Z*, and *P* forms of the conformer(s) dominant in the S_0 state.

We here analyze the TRR spectra of nondeuteriated and some deuteriated isotopomers of 2,5-DMHT using the same procedure as in ref 2. That is, we compute the T_1 vibrational frequencies of the *E*, *Z*, and *P* isomers, not only for the t,t conformer (as done for HT), but also for the t,c and c,c conformers, and we identify the excited T_n state that is responsible for the strongest $T_1 \rightarrow T_n$ transition and for the TRR activity. The Franck–Condon (FC) activity of each totally symmetric vibration in the TRR spectra in T_1 is computed for each isomer and conformer and is compared with the experimental spectrum; as we shall see, the comparison indicates unambigously which species give the largest contribution to the spectrum.

Experimental Methods

Materials. Acetonitrile-d_0 (Merck, LiChrosolv), acetonitrile-d_3 (Stohler Isotope Chemicals, 99% D), methanol (Merck, p.a.), and acetone (Merck, p.a.) were used as received. The deuteriated DMHT was prepared as described in refs 4a and 8. The deuterium incorporation was better than 95%. Throughout the transient experiments the capillaries with trienes were opened and solutions prepared and transferred to sample cells under an Ar atmosphere. Prior to the addition of triene the solvents were purged with Ar for more than 35 min.

Methods. The details of experimental procedures for recording conventional Raman and infrared spectra[9] and for time-resolved experiments[1,5] have been described previously. Briefly, the triplet state of the triene was produced by exciting acetone as sensitizer with a pump pulse from an excimer laser at 308 nm. The resonance Raman spectrum of DMHT in its T_1 state was obtained by using the second harmonic at 327.5 nm from a Nd:YAG pumped dye laser as probe pulse. The triplet-state spectra were then obtained by subtraction procedures.

Methods of Calculations

Energies, equilibrium geometries, and vibrational frequencies in the S_0 and T_1 states were computed by means of the QCFF/PI Hamiltonian,[10] which has been successfully used to predict a variety of properties of ground and excited states of conjugated molecules.[11-13] This method was used in the modified form outlined in refs 2 and 14. Energies and wave functions of triplet levels were computed by using both the QCFF/PI and the CNDO/S[15] Hamiltonians. In the latter case the electron repulsion was computed according to the Pariser relation.[16] The transition dipole moments for the $T_1 \rightarrow T_n$ transitions were also computed by both methods.

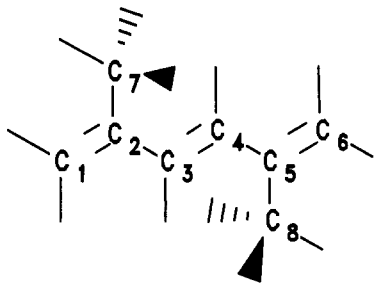

Figure 2. Numbering of atoms in DMHT.

Ground-state calculations were performed at the SCF level, while all calculations on triplet states were performed by the half-electron SCF Hamiltonian followed by a configuration interaction (CI) calculation in which all singly excited determinants with respect to the lowest triplet, belonging to the $\pi\pi^*$ space, were considered. This CI included 33 $\pi\pi^*$ determinants with two unpaired spin α electrons.

In the present QCFF/PI calculations we introduced a different set of parameters for C–CH_3 bonds, between an sp^2-hybridized carbon and an sp^3-hybridized methyl carbon atom (AB bonds, as in, for example, propene). The potential for the stretching of these types of bonds is described by the equation

$$V = \tfrac{1}{2}K_b(b - b_0)^2 - D_b$$

The original parameters ($\frac{1}{2}K_b$ = 250 kcal mol^{-1} Å^{-2}, b_0 = 1.450 Å, and D_b = 88 kcal mol^{-1}) have been replaced by the values $\frac{1}{2}K_b$ = 150 kcal mol^{-1} Å^{-2}, b_0 = 1.427 Å, and D_b = 88 kcal mol^{-1}. This modification is justified by the fact that for all methylated polyenes the previous parameters yield too high C–CH_3 stretching frequencies, in particular for compounds that contain two methyl groups on the same carbon atom or one methyl group adjacent to a C–C single bond of a polyenic chain. This set of parameters was used with success in the study of 2,5-dimethyl-2,4-hexadiene.[17]

Vibrational frequencies and normal coordinates were computed at the *E* and *Z* geometry minima of S_0 and T_1 and at the twisted geometry of T_1 (i.e., the geometry obtained by twisting the central C=C bond by 90°). All the computed frequencies are adiabatic frequencies, that is they are obtained with the energy hessian computed by also taking into account the contribution of electron density change (see ref 14).

The displacements in equilibrium geometry between the T_1 and T_n states corresponding to the strongest $T_1 \rightarrow T_n$ transition for each geometry were calculated and were used to calculate the Stokes shift parameter γ_i of each totally symmetric normal mode. The γ_i parameter, which governs the contribution to the resonance Raman spectrum of the *i*th displaced oscillator, under the condition of a predominantly Franck–Condon mechanism, is given by

$$\gamma_i = (\omega_i/2\hbar)\Delta Q_i^2$$

(6) Jacobs, H. J. C.; Havinga, E. *Adv. Photochem.* **1979**, *11*, 305.
(7) Vroegop, P. J.; Lugtenburg, J.; Havinga, E. *Tetrahedron* **1973**, *29*, 1393.
(8) Brouwer, A. M.; Cornelisse, J.; Jacobs, H. J. C. *J. Photochem. Photobiol.* **1987**, *42*, 313.
(9) Langkilde, F. W.; Amstrup, B.; Wilbrandt, R.; Brouwer, A. M. *Spectrochim. Acta* **1989**, *45A*, 883.
(10) Warshel, A.; Karplus, M. *Chem. Phys. Lett.* **1972**, *17*, 7. Warshel, A.; Karplus, M. *J. Am. Chem. Soc.* **1972**, *94*, 5612. Warshel, A.; Levitt, M. *QCPE* **1974**, *No. 247*.
(11) Warshel, A. In *Modern Theoretical Chemistry*; Schafer, H. F., III, Ed.; Plenum: New York, 1977; Vol. 7, pp 153–185.
(12) Lasaga, A. C.; Aerni, R. J.; Karplus, M. *J. Chem. Phys.* **1980**, *73*, 5230. Hemley, R. J.; Brooks, B. R.; Karplus, M. *J. Chem. Phys.* **1986**, *85*, 6550.
(13) Hudson, B.; Andrews, J. *Chem. Phys. Lett.* **1979**, *63*, 493.
(14) Zerbetto, F.; Zgierski, M. Z.; Negri, F.; Orlandi, G. *J. Chem. Phys.* **1988**, *89*, 3681.
(15) Del Bene, J.; Jaffe, H. H. *J. Chem. Phys.* **1968**, *48*, 1807.
(16) Pariser, R. *J. Chem. Phys.* **1953**, *21*, 568.
(17) Negri, F.; Orlandi, G.; Langkilde, F. W.; Wilbrandt, R. *J. Chem. Phys.* **1990**, *92*, 4907.

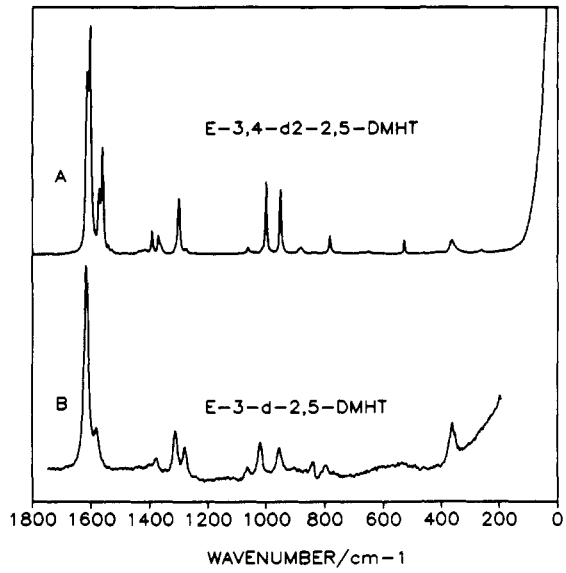

Figure 3. Ground-state Raman spectra of (A) (*E*)-DMHT-*3,4-d*$_2$ and (B) (*E*)-DMHT-*3-d*. Excitation wavelength: (A) 514.5 nm, (B) 327.5 nm.

where ω_i is the vibrational frequency (rad s^{-1}) and ΔQ_i is the projection onto the *i*th normal coordinate of T_1 of the change in equilibrium geometry between T_1 and T_n.[2] The γ parameters for torsional vibrations, the potentials of which are intrinsically anharmonic, have a clear physical meaning only for small displacements ΔQ_i, that is when the γ's themselves are small ($\lesssim$0.5).

The numbering of atoms for 2,5-DMHT is shown in Figure 2. The torsional angles of the two methyl groups were such that these molecules in the planar form belong to the C_{2h} symmetry group (Figure 2).

Results and Discussion

Experimental Results. (a) Ground State. The ground-state Raman and infrared spectra of (*E*)-DMHT have been reported previously.[18] The Raman spectrum of neat (*E*)-DMHT-*3,4-d*$_2$, excited at 514.5 nm (CW excitation), is shown in Figure 3A and the preresonance Raman spectrum of an Ar-saturated solution of 0.007 M (*E*)-DMHT-*3-d* in acetonitrile-d_3 containing 0.54 M acetone, excited at 327.5 nm (pulsed excitation), is seen in Figure 3B. The frequencies of the observed Raman and infrared bands are listed together with results from the theoretical calculations in Table V.

(b) Triplet State. The observed time-resolved resonance Raman spectra of the *E* isomers of DMHT, DMHT-*3,4-d*$_2$, and DMHT-*3-d* in the T_1 state are shown in Figure 4 and those of the *Z* isomers of DMHT and DMHT-*3,4-d*$_2$ in Figure 5. The corresponding wavenumbers are tabulated together with calculated bands in Tables IX–XI.

The spectra were obtained from the following Ar-saturated solutions: (1) 0.010 M (*E*)-DMHT in methanol and 0.82 M acetone, (2) 0.007 M (*E*)-DMHT-*3,4-d*$_2$ in acetonitrile-d_3 and 0.54 M acetone, (3) 0.007 M (*E*)-DMHT-*3-d* in acetonitrile-d_3 and 0.54 M acetone, (4) 0.011 M (*Z*)-DMHT in methanol and 0.82 M acetone, (5) 0.004 M (*Z*)-DMHT-*3,4-d*$_2$ in acetonitrile-d_3 and 0.54 M acetone. The excitation wavelength was 327.5 nm, and the delay between pump and probe pulses was approximately 60 ns in all transient experiments. All spectra shown in Figures 4 and 5 are spectra after the subtraction of solvent bands and bands from ground-state DMHT, obtained by procedures described in detail previously.[1,5] Such subtraction procedures can produce artifacts showing up as either negative bands due to the wavelength dependence of transient absorption and to depletion and/or isomerization of the starting ground-state isomer or as positive bands due to isomerization products. All spectra were carefully examined for such artifacts and the bands listed in Tables IX–XI are considered as real. Outside the regions shown in Figures 4 and 5, spectra were recorded down to 200 cm^{-1} and some weak observed bands are listed in the tables as well.

Figure 6 shows a detailed comparison of the spectra obtained from the *E* and *Z* isomers of DMHT-d_0 and DMHT-d_2. From this it is obvious that the spectra from the two isomers are different from each other.

The isomeric purity of the samples was monitored by gas chromatography throughout the experiments. We observed thermal isomerization of (*Z*)-DMHT in methanol solutions containing acetone to 1,4-dimethyl-1,3-cyclohexadiene upon storage under Ar for several days at room temperature.

Theoretical Calculations and Discussion. (a) T_1 and T_n Triplet States. Energies and wave functions of $\pi\pi^*$ triplet states of HT are given in Tables XVI–XVIII of ref 2. Since the π-electron system is the same, the nature of the $\pi\pi^*$ states in DMHT is practically the same as in HT. The lowest triplet state T_1 is dominated by the (HOMO–LUMO) singly excited configuration. The excited triplet state T_n, characterized by the largest transition moment $M(T_1,T_n)$, is T_5 in both *E* and *Z* isomers: this state lies $\sim$4.2 eV above T_1 and is dominated by the (HOMO − 1 → LUMO) and (HOMO → LUMO + 1) configurations. At the twisted geometry the T_n state with the largest $M(T_1,T_n)$ transition moment is T_6, T_7, or T_8 (depending on the rotamer) and lies 5.5 eV above T_1.

The excitation wavelength used in the TRR experiments to be discussed is λ = 327.5 nm, which corresponds closely to the T_5–T_1 energy gap in the *E* and *Z* species. Thus it is the T_5 state, or the T_n (n = 6, 7, 8) state at the twisted geometry, that is responsible for the TRR scattering and that is to be scrutinized to interpret the observed TRR spectra. It is worth noting also that while the intense T_1–T_5 transition of the *E* and *Z* forms is in resonance with the exciting photons, the correlating transition is off-resonance by $\sim$1 eV at the *P* geometry.

(b) Optimized Geometries and Energies. The energies of the different isomers of DMHT in their optimized geometries in the states S_0, T_1, and T_n are shown in Table I. The *E* forms are calculated to be the most stable in the three electronic states. The conformers of the *E* isomer (*tEt*, *tEc*, and *cEc*) are found to be almost degenerate, as their energies differ by less than 1 kcal/mol. However, the computed energies of the conformers in the ground state are not in the correct order: the calculations predict that *cEc* is the most stable conformer, while experimentally, *tEt* is the dominant one. A similar inversion of stability is also found between the *tZc* and *cZc* conformers in S_0: at variance with our results, *tZc* is found experimentally to be the most stable conformer.[4] It appears that, while the QCFF/PI Hamiltonian in general can estimate correctly nonbonded interactions, it tends to overestimate the repulsions between CH_3 groups compared to CH_2 groups and hence it "prefers" to keep the CH_3 groups far away from each other rather than the CH_2= groups.

In Tables II–IV the geometric parameters of the carbon atom backbone are given for the three states S_0, T_1, and T_n of DMHT, respectively. These results are very similar to the results obtained earlier for HT: the main differences pertain to the in-plane angle $C_2C_3C_4$, which is larger here due to steric hindrance, and to the dihedral angles $C_2C_3C_4C_5$ and $C_3C_4C_5C_6$ of the *Z* isomer, which are nonplanar in DMHT. The CC bond lengths are almost identical in the different conformers. In contrast to this, the in-plane CCC angles depend on the type of isomer; in particular,

TABLE I: Energies of Optimized Geometries (kcal/mol) of the Various Isomeric Forms Relative to the *tEt* Form in the States S_0, T_1, and T_n[a]

	S_0	T_1	T_n		S_0	T_1	T_n
tEt	0.0	0.0	0.0	*cZc*	6.4	5.4	−2.2
tEc	−0.4	0.4	−0.6	*tPt*		5.7	34.1
cEc	−0.7	0.9	0.1	*tPc*		5.9	34.7
tZt	12.6	7.1	8.9	*cPc*		6.2	36.5
tZc	8.5	5.7	3.8				

[a] n = 5, 6, 7, 8; see text.

(18) Langkilde, F. W.; Wilbrandt, R.; Nielsen, O. F.; Højgaard Christensen, D.; Nicolaisen, F. M. *Spectrochim. Acta* **1987**, *43A*, 1209.

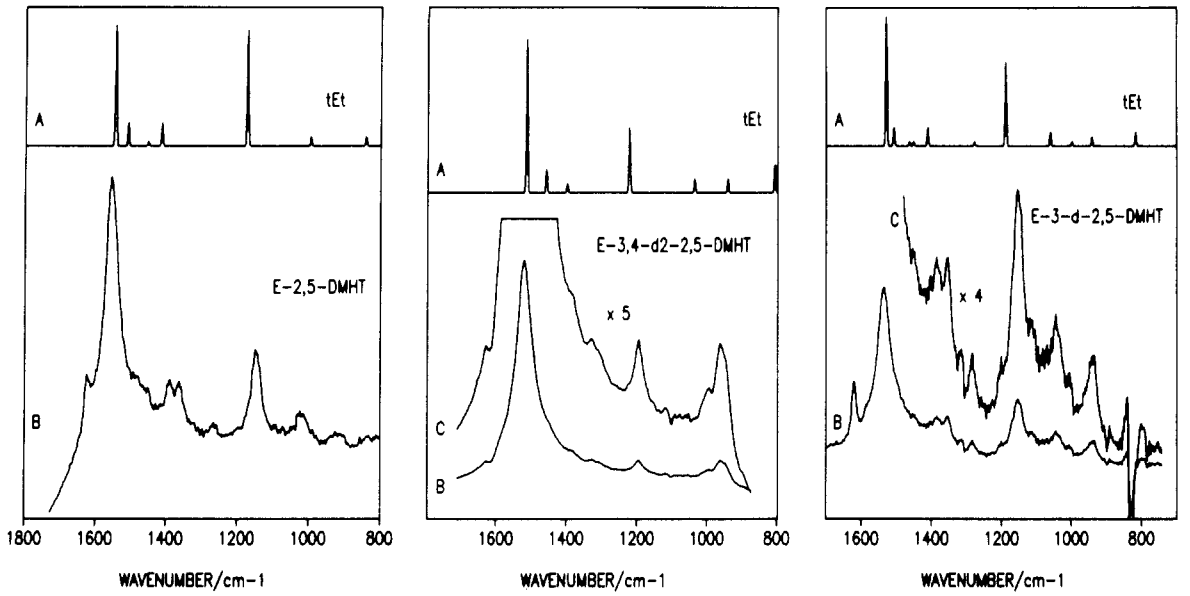

Figure 4. T_1 resonance Raman spectra of the *E* isomers of DMHT-d_0 (left), DMHT-*3,4*-d_2 (center) and DMHT-*3*-*d* (right). (A) calculated spectra for the *tEt* geometry in resonance with the $T_1 \rightarrow T_5$ transition; (B and C) experimental spectra, excitation wavelength 327.5 nm, after the subtraction of solvent and ground-state bands.

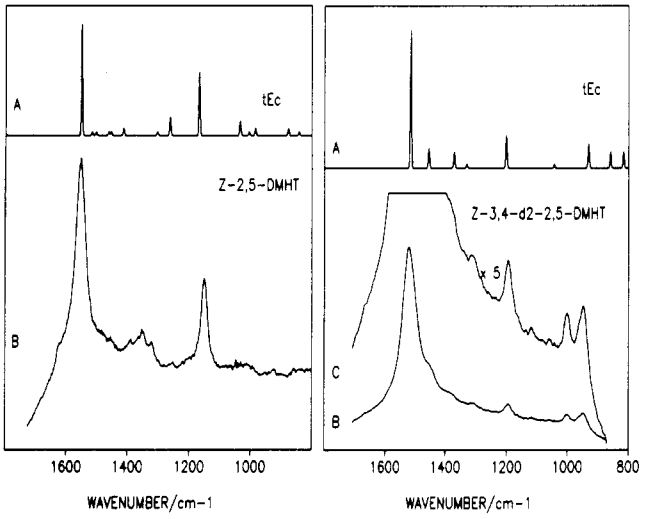

Figure 5. T_1 resonance Raman spectra of the *Z* isomers of DMHT-d_0 (left) and DMHT-*3,4*-d_2 (right). (A) Calculated spectra for the *tEc* geometry in resonance with the $T_1 \rightarrow T_5$ transition; (B and C) experimental spectra, excitation wavelength 327.5 nm, after the subtraction of solvent and ground-state bands.

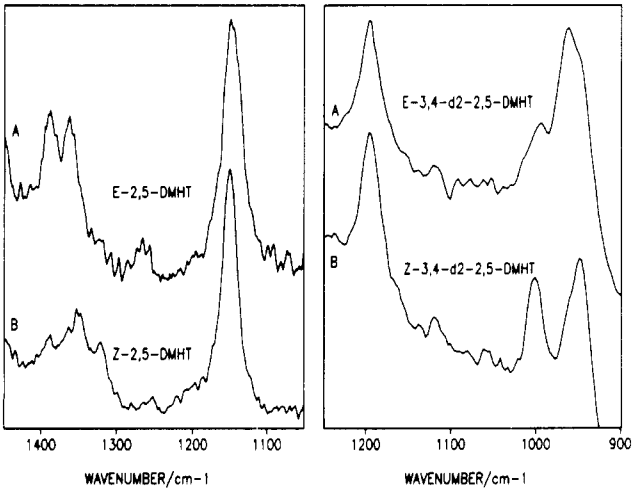

Figure 6. Comparison of the T_1 resonance Raman spectra of the *E* and *Z* isomers of DMHT-d_0 (left) and DMHT-*3,4*-d_2 (right). Conditions as for Figures 4 and 5.

TABLE II: Ground-State Geometries for the Various Isomers of 2,5-DMHT[a]

	tEt	*cEc*	*tEc*	*tZt*	*cZc*	*tZc*
C_1C_2	1.348	1.349	1.348	1.352	1.347	1.344
C_2C_3	1.481	1.479	1.481	1.480	1.478	1.484
C_3C_4	1.355	1.357	1.356	1.356	1.354	1.351
C_4C_5	1.481	1.479	1.478	1.480	1.478	1.480
C_5C_6	1.348	1.349	1.349	1.352	1.347	1.346
C_2C_7	1.499	1.500	1.499	1.488	1.501	1.499
C_5C_8	1.499	1.500	1.500	1.488	1.501	1.500
$C_1C_2C_3$	119.4	123.4	119.4	117.2	123.6	119.1
$C_2C_3C_4$	124.1	124.7	124.0	135.8	129.5	128.6
$C_3C_4C_5$	124.1	124.7	124.0	135.8	129.5	128.9
$C_4C_5C_6$	119.4	123.4	123.4	117.2	123.6	123.3
$C_1C_2C_7$	120.0	119.8	120.0	118.1	119.7	120.1
$C_6C_5C_8$	120.0	119.8	119.8	118.1	119.7	119.8
$C_1C_2C_3C_4$	179.6	358.3	179.6	174.2	330.7	144.3
$C_2C_3C_4C_5$	180.0	180.0	180.0	356.6	349.1	348.5
$C_3C_4C_5C_6$	179.6	358.3	359.5	174.2	330.7	330.4

[a] Bond lengths in Å; bond angles in degrees.

in the *Z* isomer these angles show deviations of up to 15° (especially in the ground state) with respect to the customary 120° value. Furthermore, while the *E* isomers are close to planar, the *Z* isomers are nonplanar. In the ground state torsion takes place predominantly around the CC single bonds, in the T_1 state predominantly around the central CC bond.

As in HT, the main differences caused by electronic excitation pertain to the CC bond lengths. In S_0 the CC bond lengths show the well-known alternation according to the single/double bond character of adjacent bonds. These results are in good agreement with the parameters obtained by electron diffraction.[19] Upon $S_0 \rightarrow T_1$ excitation, the double bonds lengthen and single bonds shorten, as found in the previous studies of HT. In T_π the CC bond lengths are intermediate between the values taken in S_0 and in T_1.

(c) Ground-State Vibrational Frequencies. In Table V we present the computed vibrational frequencies and the approximated description of the normal coordinates of DMHT and of its d_1 and d_2 isotopomers in the experimentally most stable conformer *tEt* of S_0. The experimental frequencies of DMHT-d_0 have been recently studied and assigned by Langkilde et al.[18] A few assignments of the weakest bands are revised here, in part on the

(19) Traetteberg, M.; Paulen, G. *Acta Chem. Scand.* **1974**, *A 281*, 1150.

TABLE III: T_1 Geometries for the Various Isomers of 2,5-DMHT[a]

	tEt	cEc	tEc	tZt	cZc	tZc	tPt	cPc	tPc
C_1C_2	1.403	1.403	1.403	1.396	1.395	1.394	1.388	1.389	1.389
C_2C_3	1.394	1.395	1.394	1.394	1.395	1.395	1.395	1.396	1.395
C_3C_4	1.473	1.471	1.471	1.481	1.480	1.481	1.483	1.483	1.483
C_4C_5	1.394	1.395	1.394	1.394	1.395	1.395	1.395	1.396	1.395
C_5C_6	1.403	1.403	1.403	1.396	1.395	1.393	1.388	1.389	1.390
C_2C_7	1.502	1.504	1.502	1.500	1.504	1.503	1.504	1.503	1.503
C_5C_8	1.502	1.504	1.503	1.500	1.504	1.504	1.504	1.503	1.503
$C_1C_2C_3$	119.6	123.7	119.6	119.0	123.7	119.5	119.8	122.8	120.0
$C_2C_3C_4$	124.0	124.7	123.9	127.3	126.7	125.6	123.9	124.1	123.5
$C_3C_4C_5$	124.0	124.7	124.8	127.3	126.7	126.0	123.9	124.1	124.1
$C_4C_5C_6$	119.6	123.7	123.7	119.0	123.7	123.4	119.8	122.8	122.8
$C_1C_2C_7$	118.7	118.4	118.7	118.2	118.6	118.6	119.1	119.1	119.2
$C_6C_5C_8$	118.7	118.4	118.5	118.2	118.6	118.7	119.1	119.1	119.1
$C_1C_2C_3C_4$	180.0	359.1	180.0	183.6	356.0	180.4	180.5	360.0	179.9
$C_2C_3C_4C_5$	180.0	177.6	180.0	300.0	305.7	297.9	268.9	269.8	90.7
$C_3C_4C_5C_6$	180.0	359.1	360.0	183.6	356.0	355.8	180.5	0.1	359.8

[a] Bond lengths in Å; bond angles in degrees.

TABLE IV: T_n Geometries for the Various Isomers of 2,5-DMHT[a]

	tEt	cEc	tEc	tZt	cZc	tZc	tPt	cPc	tPc
C_1C_2	1.417	1.418	1.416	1.417	1.418	1.419	1.421	1.416	1.416
C_2C_3	1.437	1.437	1.435	1.438	1.437	1.442	1.426	1.423	1.425
C_3C_4	1.417	1.414	1.415	1.414	1.410	1.412	1.461	1.469	1.470
C_4C_5	1.437	1.437	1.439	1.438	1.437	1.434	1.426	1.423	1.426
C_5C_6	1.417	1.418	1.418	1.417	1.418	1.414	1.421	1.416	1.419
C_2C_7	1.495	1.496	1.495	1.492	1.497	1.496	1.498	1.496	1.497
C_5C_8	1.495	1.496	1.496	1.492	1.497	1.497	1.498	1.496	1.494
$C_1C_2C_3$	118.7	122.8	118.6	117.5	123.3	117.9	118.7	122.1	119.1
$C_2C_3C_4$	123.8	124.3	124.1	130.0	128.2	127.8	123.2	125.3	121.9
$C_3C_4C_5$	123.8	124.3	124.0	130.0	128.2	127.7	123.2	125.3	123.3
$C_4C_5C_6$	118.7	122.8	122.8	117.5	123.3	122.8	118.7	122.1	122.2
$C_1C_2C_7$	119.5	119.1	119.5	118.0	118.7	118.3	119.7	119.7	119.7
$C_6C_5C_8$	119.5	119.1	119.2	118.0	118.7	119.0	119.7	119.7	119.2
$C_1C_2C_3C_4$	180.0	358.4	180.0	171.2	338.2	165.3	180.3	0.00	179.9
$C_2C_3C_4C_5$	180.0	179.3	180.0	337.1	339.7	336.2	269.8	270.0	90.7
$C_3C_4C_5C_6$	180.0	358.4	360.0	171.2	338.2	338.6	180.3	0.00	359.8

[a] Bond lengths in Å; bond angles in degrees.

basis of a comparison with (*E*)-2-methyl-1,3,5-hexatriene and (*E*)-4-deuterio-2-methyl-1,3,5-hexatriene.[9] The agreement between computed and observed in-plane frequencies is quite satisfactory. In particular, the present calculations confirm the coupling between the polyenic C–C single bond stretch and the C–CH_3 stretch vibration, suggested by Langkilde et al.,[18] which leads to a repulsion between the two frequencies. It is worth noting that the updating of the parameters describing the C–CH_3 potential, discussed above, is instrumental in improving the agreement between the experimental and theoretical frequencies of C–CH_3 vibrations.

The list of the experimental out-of-plane frequencies is not complete, mainly because the low-frequency (below 530 cm^{-1}) range was not explored by IR spectroscopy. The agreement between computed and observed out-of-plane frequencies is satisfactory.

(d) T_1 Vibrational Frequencies. In Table VI we report the T_1 frequencies of the d_0, d_1, and d_2 isotopomers of the *tEt* conformer. The $S_0 \rightarrow T_1$ excitation affects mainly the force field of the C=C and C—C stretches and torsions. Thus, most of the differences between the T_1 and S_0 frequencies are noted in the range $\geq$1100 cm^{-1}. At the same time, normal coordinates, especially for modes of CC character, undergo a mixing (Duschinsky effect) when passing from S_0 to T_1. Comparing the T_1 frequencies of DMHT with those of the parent molecule HT, we note that most frequencies of the latter show up virtually unchanged also in DMHT, where they are intermingled with the frequencies pertinent to the CH_3 groups.

In Table VI we report also the γ parameters that were defined above. Since these parameters are proportional to the Franck–Condon intensity of the corresponding fundamentals in the TRR spectra, they are essential for the interpretation of these spectra. The modes with nonzero γ are the a_g modes and the largest γ values are associated with the vibrations at 1545, 1173, and 304 cm^{-1} in DMHT-d_0. Hence, as it might have been anticipated, the computed γ are quite similar to the γ found for HT. The effect of deuteriation is that of introducing some redistribution among the γ parameters as a consequence of the normal coordinate mixing.

In Tables VII and VIII we show the T_1 frequencies and the γ parameters for the $T_1 \rightarrow T_n$ transition of the conformers *tEc* and *cEc* in the isotopomers d_0 and d_2. The changes in the list of the frequencies compared with those of the *tEt* conformer are rather small; however, modifications are found in the normal coordinates and these are reflected in the values of the γ's, especially for the frequencies in the region around 1100 cm^{-1}. The results for the *tEc* conformer show a further difference with respect to the *tEt* conformer because in *tEc* the center of symmetry is lost, the distinction between the g and u symmetry labels becomes meaningless, and thus, vibrations of b_u parentage (at 1278 and 941 cm^{-1}) may acquire intensity.

The full list of frequencies and γ parameters of the *tZt*, *tZc*, *cZc*, *tPt*, *tPc*, and *cPc* forms are not reported here, but are available as supplementary material. In the next section, those frequencies with the largest γ's will be reported and discussed.

(e) Comparison between Computed and Observed Spectra. In this section we compare the frequencies and the intensities of the bands appearing in the TRR spectra with the computed frequencies and the γ parameters of T_1 normal vibrations of each conformer for the three *E*, *Z*, and *P* isomers. The availability of deuteriated isotopomers adds more strength to the proposed assignments.

TABLE V: Ground-State Vibrational Frequencies of the *tEt* Form of 2,5-DMHT and Its d_2 and d_1 Isotopomers

d_0			d_2		d_1	
calc ω	description	exp ω	calc ω	exp ω	calc ω	exp ω
		sym, A_g				
1665	C=C	1624	1648	1613/1603	1657	1616
1598	C=C	1590/1575	1572	1573/1561	1587	1581
1468	CH_3 def	1458	1467		1467	
1447	CH_3 def, CH_2 sciss	1373	1446	1371	1446	1377
1422	CH_2 sciss, CH_3 def	1398	1422	1393	1422	1311
1376	C—C, C—CH_3, CH rock	1315/1304	1354	1300	1362	1278
1340	CH rock, C—CH_3, C—C	1295	1095		1082	1060
1028	CH_3 rock	1032	1020	1000	1021	1019
992	CH_2 rock	971	934	952	939	955
844	C—CH_3	846	799	746	810	840
606	CCC def	538	600	528	603	795
392	CCC def	367	392	363	392	359
303	CCC def	271	302		303	
		sym, A_u				
1476	CH_3 def		1476	1443	1476	
1062	CH_3 rock	1038	1061		1062	
1018	CH wag	991	768	750	942	
952	CH_2 wag	882	952	885	954	
739	CH_2 twist	716	721	685/682	738	
509	CC wag		506		508	
214	C—CH_3 twist		213		213	
137	C=C twist		134		135	
56	C—C twist		56		56	
		sym, B_u				
1650	C=C	1616	1647	1621/1619	1647	
1468	CH_3 def	1453	1468	1453	1468	
1453	CH_2 sciss	1433	1446	1423	1449	
1435	CH_3 def	1373	1433	1377	1434	
1370	C—CH_3, C—C, CH rock	1309	1334	1310/1303	1357	
1293	CH rock, C—CH_3, C—C	1254	1046		1310	
1024	CH_3 rock	1007	1023	1003	1024	
965	CH_2 rock	960	943	958	973	
853	C—CH_3	842	823	784	849	
584	CCC def	536	561	535	571	
515	CCC def		513		514	
160	CCC def		158		159	
		sym, B_g				
1476	CH_3 def	1438	1476	1435	1476	
1061	CH_3 rock		1060	1063/1035	1060	
952	CH_2 wag	888	952	882	952	
868	CH wag		786	783	782	
724	CH_2 twist		696	651	700	
438	CC wag	443/422	424	417	430	
202	C—CH_3 twist	212	202	192	202	
193	C—C twist		166	140	178	

According to the NEER principle, ground-state conformations at C–C single bonds are preserved upon excitation to the excited T_1 state. On this basis the dominant ground-state *tEt* conformer may, after equilibration with respect to torsion around the central CC bond, in the T_1 state lead to *tEt*, *tZt*, or *tPt* geometries. Correspondingly, the dominant ground-state *tZc* conformer may lead to the *tEc*, *tZc*, or *tPc* triplet geometries. We shall in the following discuss the experimental TRR spectra along these lines. It should be noticed that the validity of the NEER principle rests on the short lifetime (~100 ns for (*E*)-DMHT[5]) and high energy barrier (>8 kcal/mol for DMHT[5]) of the rotation around CC single bonds in the T_1 state.

In the case of HT the conformer *tXt* (X = *E*, *Z*, *P*) is much more stable than the other conformers for both the *E* and the *Z* isomers in the ground state. The TRR spectra of *E* and *Z* isomers are identical and this agrees with the notion that also in T_1 the conformer *tXt* is the dominant one in each geometric isomer. In DMHT the situation is more complicated as the energies of the different conformers are rather similar. Experimentally, in S_0 the prevailing *E* conformer is *tEt*, while the dominant *Z* conformer is *tZc*. Furthermore, in the time-resolved experiments, the T_1 spectra of the *E* and *Z* isomers are similar but different: this observation can be explained on the basis of the different conformer prevailing in the *E* and *Z* isomer in S_0 and by assuming that the conformer distribution of S_0 is adopted in T_1 (NEER principle).

In Table IX we compare the experimental T_1 spectrum of the d_0, d_1, and d_2 isotopomers of the *E* species with the theoretical results for the *tEt*, *tPt*, and *tZt* conformers of the same species.

We recall that the *tZt* conformer is computed to be 7.1 kcal/mol higher in energy than *tEt* and thus it is not expected to contribute significantly to the TRR spectra of the *E* isomer of DMHT. Furthermore, the *tPt* species is calculated to be off-resonance by ~1 eV with respect to the excitation wavelength.

The T_1 spectrum of (*E*)-DMHT-d_0 is composed of two intense bands at 1551 and 1146 cm^{-1} and weak bands at 1389, 1357, 1266, 1016, and 916 cm^{-1}. The spectrum computed for *tEt* corresponds well to the observed spectrum, although the calculated intensity of the band at 1335 cm^{-1} is too low. We note that for this geometry a band of medium intensity is calculated at 304 cm^{-1}. This band was indeed observed at 360 cm^{-1} in experiments performed at 188 K (not reported here). The spectrum computed for *tPt* does not match even the main features of the observed spectrum. The spectrum calculated for *tZt* predicts correctly the main observed bands, but it also predicts very strong bands at 462, 321, and 260 cm^{-1}, which are not observed experimentally.

The observed T_1 spectrum of (*E*)-DMHT-d_2 differs from the spectrum of the nondeuteriated species in that the intense band

TABLE VI: Computed Wavenumbers (cm^{-1}) in the T_1 State and Stokes Shift Parameters γ^a for the T_1–T_n Transition of (*tEt*)-2,5-DMHT and Its Deuteriated Forms

d_0			3,4-d_2		3-d_1	
ω	description	γ	ω	γ	ω	γ
		sym, A_g				
1545	C—C, C=C	0.26	1513	0.33	1529	0.28
1509	CH_2 sciss, C=C	0.05	1503		1507	0.04
1466	CH_3 def		1457	0.05	1463	0.01
1452	CH_3 def	0.01	1446		1451	0.01
1413	C—CH_3, C—C	0.05	1398	0.02	1411	0.04
1335	CH rock, C=C		1035	0.03	1060	0.03
1173	C=C, CH rock	0.25	1222	0.14	1189	0.18
1009	CH_3 rock		1004		1008	
995	CH_2 rock	0.02	940	0.03	998	0.01
841	C—CH_3, C—C	0.02	806	0.06	816	0.03
595	CCC bend	0.02	588	0.01	593	0.01
383	CCC bend	0.02	383	0.02	383	0.02
304	CCC bend	0.13	303	0.12	303	0.12
		sym, A_u				
1477	CH_3 def		1476		1476	
1056	CH_3 rock		1056		1056	
856	CH wag		660		828	
766	CH_2 wag		773		764	
572	CH_2 twist		564		572	
487	CC wag		472		484	
213	C—CH_3 twist		212		212	
115	C—C twist		114		114	
65	C=C twist		63		64	
		sym, B_u				
1495	CH_2 sciss, C=C, C—C		1494		1494	
1464	CH_3 def		1464		1464	
1451	CH_3 def		1446		1446	
1412	C—CH_3, C—C		1395		1395	
1390	C—C, CH rock		1316		1368	
1241	CH rock, C=C		1075		1278	0.01
1005	CH_2 rock		940		941	0.02
991	CH_3 rock		992		991	
847	C—CH_3, C—C		828		845	
598	CCC bend		573		583	
508	CCC bend		506		507	
162	CCC bend		160		161	
		sym, B_g				
1476	CH_3 def		1476		1476	
1056	CH_3 rock		1056		1056	
802	CH wag		678		671	
761	CH_2 wag		772		772	
569	CH_2 twist		558		560	
469	CC wag		438		447	
301	C—C twist		278		290	
205	C—CH_3 twist		205		205	

[a] Only γ values ≥0.01 are reported.

TABLE VII: Computed Wavenumbers (cm^{-1}) in the T_1 State and Stokes Shift Parameters γ^a for the T_1–T_n Transition of (*tEc*)-2,5-DMHT and Its Deuteriated Forms

d_0			3,4-d_2	
ω	description	γ	ω	γ
		sym, A′		
1549	C—C, C=C	0.30	1515	0.34
1515	CH_2 sciss, C=C	0.01	1506	
1501	CH_2 sciss, C—C,C=C	0.01	1498	
1469	CH_3 def, CH_2 sciss		1466	
1460	CH_3 def	0.01	1455	0.05
1452	CH_3 def	0.01	1449	
1451	CH_3 def, CH_2 sciss		1442	
1424	C—CH_3, CH rock, CH_3 def		1408	
1412	C—C, C—CH_3, CH_3 def	0.02	1372	0.04
1369	C—C, C=C		1331	0.01
1303	C—C, C=C, CH rock	0.01	1044	0.01
1262	C—C, C=C, CH rock	0.05	931	0.06
1166	C=C	0.17	1202	0.08
1033	CH_2 rock, CH_3 rock	0.04	1065	
1004	CH_3 rock, CH_2 rock	0.01	1006	
995	CH_2 rock		993	
984	CH_3 rock	0.02	948	
877	C—C, C—CH_3	0.02	859	0.04
842	C—CH_3, C—C	0.01	817	0.04
604	CCC bend	0.01	582	
581	CCC bend		569	
514	CCC bend		512	
371	CCC bend	0.02	370	0.02
320	CCC bend	0.05	318	0.04
164	CCC bend	0.14	163	0.14
		sym, A″		
1477	CH_3 def		1477	
1473	CH_3 def		1473	
1056	CH_3 rock		1056	
1056	CH_3 rock		1056	
849	CH wag		657	
793	CH wag		676	
769	CH_2 wag		770	
761	CH_2 wag		771	
570	CH_2 twist		561	
567	CH_2 twist		551	
491	CC wag		480	
472	CC wag		442	
291	C—C twist		268	
209	C—CH_3 twist		209	
171	C—CH_3 twist		171	
110	C—C twist		109	
63	C=C twist		61	

[a] Only γ values ≥0.01 are reported.

at 1146 cm^{-1} is replaced by four medium-intensity bands at 1195, 994, 958, and 945 cm^{-1}. The spectrum computed for *tEt* corresponds closely to the observed spectrum since it reproduces the intense band at 1519 cm^{-1} and the intensity redistribution in the region 1200–900 cm^{-1}. The spectrum computed for the *tPt* species does not match the observed spectrum because the band calculated at 1389 cm^{-1} comes out too strong, as intense as the calculated 1511-cm^{-1} band, and no intense band is computed around 1000 cm^{-1}. Also the spectrum computed for the *tZt* conformer is unsatisfactory, since the intensities of the 1519- amd 1195-cm^{-1} bands are not estimated correctly and no bands around 1000 cm^{-1} are predicted. Moreover, strong bands are calculated for *tZt* at 432, 309, and 251 cm^{-1}, which are not observed experimentally.

The observed spectrum of (*E*)-DMHT-d_1 shows a richer structure than (*E*)-DMHT-d_0. Beside the intense band at 1537 cm^{-1}, it shows medium-intensity bands at 1354, 1154, and 938 cm^{-1}. Due to the isotopic substitution of a single H atom, the symmetry of the kinetic part of the vibrational Hamiltonian is lower than in the parent species and the distinction between g and u vibrations is meaningless. The spectrum computed for *tEt* accounts for the main features of the observed TRR spectrum: in particular, it explains the observed bands quoted above as due to the 1529-, 1411-, 1189-, and 941-cm^{-1} vibrations. Interestingly, two of the observed bands are attributed to in-plane modes of b_u parentage that acquire intensity via mixing with vibrations of a_g parentage. The spectrum computed for the *tPt* conformer overestimates the intensity and the number of bands in the 1400-cm^{-1} frequency region. The spectrum computed for the *tZt* species lacks the counterpart of the band observed at 1354 cm^{-1} and overestimates the intensity of the 1154-cm^{-1} band. Moreover, strong calculated bands for *tZt* at 436, 311, and 255 cm^{-1} are not observed experimentally.

It follows that the TRR spectra of the three isotopomers of (*E*)-DMHT species are well represented by the spectra computed for the *tEt* conformer, whereas the spectra computed for the *tPt* and *tZt* conformers cannot be reconciled with the observed spectra. The calculated *tEt* spectra of the three isotopomers of (*E*)-DMHT are shown in Figure 4 together with the corresponding experimental spectra.

The T_1 spectra of the d_0 and d_2 isotopomers of the (*Z*)-DMHT species are compared in Table X with the theoretical results obtained for the *tEc*, *tPc*, and *tZc* conformers of the same isotopomers and in Table XI with the results pertaining to the *cEc*, *cPc*, and *cZc* conformers. We recall that, experimentally, the *tZc* conformer is more stable than the *cZc* conformer in S_0 and then,

TABLE VIII: Computed Wavenumbers (cm^{-1}) in the T_1 State and Stokes Shift Parameters γ^a for the T_1–T_n Transition of (*cEc*)-2,5-DMHT and Its Deuteriated Forms

	d_0		3,4-d_2	
ω	description	γ	ω	γ
	sym, A_g			
1552	C—C, C=C	0.32	1518	0.33
1506	CH_2 sciss		1505	0.01
1457	CH_3 def		1455	0.01
1447	CH_3 def	0.01	1444	
1425	C=C, C—CH_3, CH_3 def		1390	0.07
1302	CH rock, C—CH_3	0.08	935	0.07
1170	C=C	0.09	1193	0.06
1045	C—C, C=C, CH_3 rock	0.13	1077	0.07
1005	CH_2 rock	0.04	1008	
892	C—CH_3, C=C	0.03	865	0.13
577	CCC bend		570	
363	CCC bend	0.02	362	0.02
333	CCC bend	0.01	332	0.01
	sym, A_u			
1475	CH_3 def		1471	
1038	CH_3 rock		1037	
842	CH wag		654	
769	CH_2 wag		771	
566	CH_2 twist		553	
496	CC wag		487	
174	C—CH_3 twist		173	
106	C—C twist		104	
59	C=C twist		58	
	sym, B_u			
1520	CH_2 sciss, C=C, C—C		1507	
1463	CH_3 def, CH_2 sciss		1460	
1455	CH_3 def		1451	
1425	C—CH_3, C—C, CH_3 def		1409	
1358	C—C, C=C, CH rock		1300	
1228	CH rock, C=C, C—CH_3		944	
1013	CH_2 rock		1043	
993	CH_3 rock		997	
856	C—CH_3, C=C		854	
596	CCC bend		570	
519	CCC bend		516	
168	CCC bend		167	
	sym, B_g			
1475	CH_3 def		1475	
1037	CH_3 rock		1037	
783	CH wag		656	
772	CH_2 wag		774	
567	CH_2 twist		549	
481	CC wag		452	
282	C—C twist		260	
166	C—CH_3 twist		165	

[a] Only γ values ≥0.01 are reported.

on the basis of the NEER principle, the *tXc* conformers are expected to be the species that contribute most to the observed TRR spectra originating in T_1.

The T_1 spectrum of the (*Z*)-DMHT-d_0 species is formed by two intense bands at 1548 and 1151 cm^{-1} and by weak bands at 1392, 1350, 1320, 1252, 1004, and 927 cm^{-1}. The intensity computed for the modes of the *tEc* conformer represents quite satisfactorily the observed spectrum. The spectrum computed for the *tPc* species lacks the intense band at 1151 cm^{-1} and underestimates the intensity of the CC stretch at 1548 cm^{-1}. The spectrum computed for the *tZc* rotamer is slightly better, but here, the intensity associated to the 1548-cm^{-1} band is split among a number of modes and strong calculated bands at 469 and 315 cm^{-1} are not observed experimentally.

The calculation on the *cXc* conformers leads to TRR spectra that are less satisfactory than the spectra obtained for *tXc* conformers. In particular, these spectra do not represent correctly the observations in the range 900–1200 cm^{-1}.

The T_1 spectra of (*Z*)-DMHT-d_2 are composed of an intense band at 1519 cm^{-1} and of a number of medium-intensity bands at 1195, 1000, and 960/949 cm^{-1}. The spectrum computed for the *tEc* conformer represents rather well the observed spectrum. The spectra computed for the other two isomers, *tPc* and *tZc*, are substantially different from the experimental spectrum, as it can be seen in Table X. Among the *cXc* conformers, only the spectrum for the *cEc* species reproduces reasonably well the TRR spectrum of (*Z*)-DMHT-d_2.

TABLE IX: Experimental Frequencies (cm^{-1}) of the Bands Active in the TRR Spectra of *E* Species for the d_0, d_2, and d_1 Isotopomers of DMHT Compared with the Theoretical Results for *tXt* Conformers

exp		*tEt*		*tPt*		*tZt*	
ω	*I*	ω	γ	ω	γ	ω	γ
		DMHT-d_0					
1551	s	1545	0.26	1514	0.19	1496	0.28
		1509	0.05	1478	0.04	1464	0.07
1389	w	1452	0.01	1404	0.13	1406	0.03
1357	w	1413	0.05	1300	0.07	1280	0.12
1266	w	1335	0.0				
1146	m	1173	0.25	1155	0.03	1148	0.34
1016	w	995	0.02	1006	0.01		
916	w	841	0.02	961	0.01	937	0.02
						462	0.67
		304	0.13			321	0.74
						260	0.87
		DMHT-d_2					
1519	s	1513	0.33	1511	0.20	1504	0.02
1451	sh	1457	0.05	1438	0.05	1492	0.19
1384	w	1398	0.02	1389	0.13	1486	0.03
1329	w					1459	0.13
1195	m	1222	0.14	1245	0.06	1233	0.39
1119	w						
994	m	1035	0.03				
958	m	940	0.03	952	0.01		
945	sh	806	0.06	801	0.06	860	0.13
						432	0.52
		303	0.12			309	0.73
						251	1.43
		DMHT-d_1					
1537	s	1529	0.28	1513	0.11		
		1507	0.04	1511	0.09	1495	0.26
1383	w	1451	0.01	1448	0.03	1461	0.07
1354	m	1411	0.04	1404	0.05		
1315	w			1388	0.06		
1284	w	1278	0.01 b_u	1298	0.05		
1154	m	1189	0.18	1215	0.04	1220	0.34
1040	w	1060	0.03				
1005	w	998	0.01				
938	m	941	0.02 b_u	958	0.01	909	0.06
						436	0.40
						311	0.47
						255	1.14

It follows that the T_1 spectra of the d_0 and d_2 isotopomers of (*Z*)-DMHT are represented satisfactorily only by calculations for the *tEc* species. Theoretical spectra for the *P* and *Z* isomers are clearly less satisfactory; furthermore, TRR spectra are reproduced better by calculation on the *tEc* than on the *cEc* conformer. This fact agrees with the observation that in S_0, the *Z* form exists predominantly as the *tZc* conformer. The calculated *tEc* spectra are shown in Figure 5 together with the experimental spectra of the *Z* isomers of DMHT-d_0 and DMHT-d_2.

As the previously reported T_1 spectra of (*E*)- and (*Z*)-DMHT showed rather small differences they were remeasured in methanol in the present work. In Figure 6 characteristic regions of the spectra of the two isomers of DMHT-d_0 and DMHT-d_2 are shown. From Figure 6 it is seen clearly that differences are observed in the T_1 spectra of the two isomers from both isotopomers, in particular with respect to intensities but also to frequencies.

Having assigned the observed TRR spectra of (*E*)-DMHT and (*Z*)-DMHT to the *tEt* and *tEc* species, respectively, we now give a qualitative description of the normal modes that contribute most to the spectra. The intense bands at 1520–1550 cm^{-1} can be assigned to a combination of C=C and C—C stretches, as shown in Tables VI and VII. Their intensity can be explained in terms of the large CC bond length change between T_1 and T_n. The other

TABLE X: Experimental Frequencies (cm^{-1}) of the Bands Active in the TRR Spectra of *Z* Species for the d_0 and d_2 Isotopomers of DMHT, Compared with the Theoretical Results for *tXc* Conformers

exp		*tEc*		*tPc*		*tZc*	
ω	*I*	ω	γ	ω	γ	ω	γ
		DMHT-d_0					
1548	s	1549	0.30	1533	0.10	1531	0.14
				1512	0.06	1488	0.12
1392	w	1412	0.02	1402	0.05	1459	0.05
						1447	0.03
1350	w	1369	0.00	1296	0.03	1299	0.06
1320	w	1303	0.01	1251	0.02	1248	0.03
1252	w	1262	0.05				
1151	m	1166	0.17			1141	0.33
1004	w	1033	0.04	1005	0.04		
927	w	877	0.02	968	0.06	946	0.09
						488	0.17
						469	0.61
		320	0.05			315	1.35
		DMHT-d_2					
1519	s	1515	0.34	1520	0.09	1517	0.13
				1509	0.05	1485	0.11
1455	sh	1455	0.05	1453	0.03	1455	0.08
						1437	0.06
1388	w	1372	0.04	1387	0.03	1383	0.03
				1384	0.05		
1311	w	1331	0.01				
1195	m	1202	0.08			1213	0.35
1118	w	1044	0.01				
1000	m	931	0.06	1006	0.02		
960	sh	859	0.04	959	0.08	946	0.05
949	m	817	0.04			855	0.17
						437	0.61
						297	1.79

TABLE XI: Experimental Frequencies (cm^{-1}) of the Bands Active in the TRR Spectra of *Z* Species for the d_0 and d_2 Isotopomers of DMHT, Compared with the Theoretical Results for *cXc* Conformers

exp		*cEc*		*cPc*		*cZc*	
ω	*I*	ω	γ	ω	γ	ω	γ
		DMHT-d_0					
1548	s	1552	0.32	1540	0.16	1533	0.31
						1491	0.08
1392	w	1447	0.01			1435	0.05
1350	w						
1320	w	1302	0.08	1249	0.05		
1252	w						
1151	m	1170	0.09			1138	0.30
1004	w	1045	0.13				
927	w	1005	0.04	984	0.10	948	0.05
						494	0.65
				342	0.07	314	0.86
		DMHT-d_2					
1519	s	1518	0.33	1527	0.15	1522	0.28
						1491	0.09
1455	sh	1455	0.01	1468	0.04	1471	0.05
						1435	0.05
1388	m	1390	0.07	1388	0.03	1383	0.05
1311	w						
1195	m	1193	0.06			1185	0.19
1118	w	1077	0.07				
1000	m	1008	0.00	1038	0.03		
960	sh						
949	m	935	0.07	967	0.07		
		865	0.13			460	0.60
				327	0.11	297	1.09

strong band, at ca. 1150 cm^{-1} in nondeuteriated compounds, is assigned to the central C=C stretch; its frequency is considerably lowered with respect to the ground state because of its decreased bond order upon $S_0 \rightarrow T_1$ excitation and its intensity is due to the change in the bond length observed in the $T_1 \rightarrow T_n$ excitation. Deuteriation leaves the higher frequency band unaltered, but splits the lower frequency band into a number of bands: this observation is understood as due to the mixing of the central CC stretch with CD rocks with the effect of pushing the frequency with dominant CC character up to ca. 1200 cm^{-1}.

We shall now discuss the reasons why the *E* isomer is the only one responsible for the T_1 TRR spectra. The absence of contributions from the *Z* isomer is attributed to its negligible population in the equilibrated T_1 triplet, due to its relatively high steric energy and to the freedom of the molecule to rotate around the central CC bond. The lack of indications of the *P* form in the TRR spectra cannot be attributed simply to its low population. First of all, the energy of the *P* form is similar to, and according to some calculations even lower than, the energy of *E* isomer. (As discussed previously,[17] QCFF/PI tends to overestimate energies of twisted geometries.) Furthermore, there is at least a second reason for the lack of bands attributable to the *P* isomer: as discussed above, RR scattering in the experiments discussed is of preresonance (PR) character in the *P* form, but of resonance type in the *E* or *Z* form. The photon energy of the probing light used in these experiments matches the T_1–T_5 energy gap in the planar forms, but is lower than the computed T_1–T_n energy gap of the intense triplet–triplet transition in the *P* form.[2,3]

In the following, we estimate the ratio between the Raman scattering efficiencies of the *E* and *P* forms in order to assess their population ratio from the observed spectra. We consider for simplicity a model based on a single mode. The intensity of the PR Raman effect is[20]

$$I_{PR} = \frac{4M_{1n}^4\omega^2\gamma(E_{1n}^2 + \Omega^2 + E_{1n})^2}{E_{1n}^2 - \Omega^2}$$

where γ is the displacement parameter of the active mode, ω is its frequency, M_{1n} and E_{1n} are the transition moment and the energy difference, respectively, between T_1 and T_n triplets, and Ω is the exciting photon energy.

The intensity of RR scattering, when the exciting photons are in resonance with the 0–0 band of $T_1 \rightarrow T_n$ transition, is[20]

$$I_{RR} = (\gamma e^{-2\gamma}/\Gamma^2)M_{1n}^4$$

where Γ is the homogeneous line width of the 0–0 band.

In the T_1 spectra of DMHT, the scattering of planar molecules is in-resonance and that of twisted molecules is off-resonance by ca. 1 eV, as can be deduced from the T_1–T_n excitation energies at different geometries (vide supra). The electronic transition moments are roughly the same in the two cases[2] and this holds also for the γ parameter of the most active mode. Thus the model parameters we adopt are as follows: $E_{1n} = 32\,000$ cm^{-1} (in resonance), $\Omega = 32\,000$ cm^{-1}, $E_{1n} = 40\,000$ cm^{-1} (preresonance), $\gamma = 1.0$, $\omega = 1600$ cm^{-1}, $\Gamma = 300$ cm^{-1}. M_{1n} is taken to be the same for both RR and PR scattering. With these parameters we get a ratio of scattering intensities $I_{RR}/I_{PR} = 2000$. Thus, with the laser excitation wavelength used, the scattering activity of *E* isomers is ~2000 times larger than the activity of the *P* isomers. In these TRR spectra no band belonging to the *P* form was identified; hence the most intense among such bands can be assumed to be at least 20 times weaker than the strongest band of the *E* form. In view of the different scattering efficiency of the two isomers, the dominance of the *E* isomer in the TRR spectra is compatible with a population ratio $N_E/N_P \gg 0.01$. With use of the Boltzmann relation and room temperature, this ratio suggests that the *P* form cannot be lower by more than ~2.7 kcal/mol (depending on the number of distinct species) than the *E* isomer.

A qualitative representation of the T_1 PES of the *tXt* conformer of DMHT, along the torsion around the central CC bond, based on the above discussion, is shown in Figure 7. For comparison with unsubstituted 1,3,5-hexatriene, the reader is referred to Figure

(20) Siebrand, W.; Zgierski, M. Z. *J. Chem. Phys.* **1979**, *71*, 3561.
(21) Arai, T.; Karatsu, T.; Sakuragi, H.; Tokumaru, K. *Tetrahedron Lett.* **1983**, *24*, 2873. Arai, T.; Karatsu, T.; Misawa, H.; Kuriyama, Y.; Okamoto, H.; Hiresaki, T.; Furuuchi, H.; Zeng, H.; Sakuragi, H.; Tokumaru, K. *Pure Appl. Chem.* **1988**, *60*, 989.
(22) Sandros, K.; Becker, H.-D. *J. Photochem.* **1987**, *39*, 301.
(23) Yee, W. A.; Hug, S. J.; Kliger, D. S. *J. Am. Chem. Soc.* **1988**, *110*, 2164.

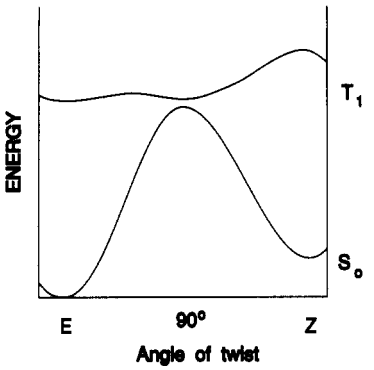

Figure 7. Qualitative potential energy surface of the *tXt* conformer of DMHT in the T_1 and S_0 states along the torsion of the central CC bond. See text for discussion.

10 of the previous paper in this issue. (It should be mentioned that the PES for the *cXt* conformer of DMHT differs somewhat from the picture given in Figure 7; this will be the subject of future work.) In both DMHT and HT the *E* and twisted minima are roughly at the same energy (within less than 1 kcal/mol) and are separated by a barrier sufficiently low to allow equilibration during the T_1 lifetime. Both forms are substantially populated. The *Z* form is quasi-degenerate with the *E* form in HT, but is considerably higher, by 5–7 kcal/mol, in DMHT because of steric repulsion. Thus, at room temperature, the population of the *Z* form is negligible in DMHT, but substantial in HT.

Only the planar forms (only the *E* form in DMHT) contribute to the transient RR spectra. The twisted form does not contribute significantly, since the exciting wavelength is off-resonance with respect to the intense $T_1 \rightarrow T_n$ transition. However, at the twisted form the T_1 deactivation does take place, because of the small energy gap to the ground state. In this respect the situation is similar to the one prevailing in naphthylethylene,[24] where the transient T–T absorption from T_1 is mostly due to the planar forms, while the deactivation takes place at the perpendicular form.

Conclusion

We have interpreted the T_1 resonance Raman spectra of DMHT and of its deuteriated isotopomers and we have assigned them to the *E* form of the conformers prevailing in each of the *E* and *Z* isomers in the equilibrated ground state.

The lack of observation of bands belonging to the *Z* form is explained in terms of nonbonded interactions, which lead to a higher energy than in the *E* form and hence to a smaller population in the thermally equilibrated triplet. The lack of contributions to the T_1 TRR spectra from the *P* form is attributed in part to its smaller scattering efficiency, due to its preresonance character, in comparison with the in-resonance character of the scattering from the *E* isomer. An estimate of the ratio between the scattering activities of the two forms leads to a lower limit for the population ratio N_E/N_P of 0.01. This indicates that the relative minimum in the T_1 potential energy curve found by some calculations at the twisted geometry is lower than the *E* energy by at most 2.7 kcal/mol.

A comparison with the previously discussed case of parent 1,3,5-hexatriene indicates that while the potential energy surface of 1,3,5-hexatriene shows nearly isoenergetic minima at planar *E* and *Z* geometries, the introduction of methyl groups in 2- and 5-positions causes considerable distortion of the T_1 surface. In particular, the energy of planar (*Z*)-DMHT is raised by nonbonded interaction. Furthermore, steric interaction leads to a change in C–C single bond conformation in both the S_0 and T_1 when going from HT to DMHT. The influence of these changes on the quantum yields of $E \rightarrow Z$ and $Z \rightarrow E$ isomerization is yet to be investigated.

For aryl-substituted ethylenes,[21,22] the terms one-way and adiabatic isomerization have been discussed previously. In the present case of 2,5-DMHT, a simple alkyl-substituted polyene, one-way $Z \rightarrow E$ isomerization takes place on the T_1 PES by rapid equilibration. This is then followed by decay to the S_0 PES via the perpendicular geometry. Since at this geometry, a maximum is found on the S_0 PES, the molecules relax to both planar *E* and *Z* S_0 geometries, thus giving rise to diabatic photoisomerization. The present results show that it is possible to sterically influence the detailed shape of the potential energy surfaces in excited states. As the release of strain occurs along different coordinates in excited states than in the ground state, the reactivity of excited-state molecules may be influenced in different ways than in the ground state.

Acknowledgment. This work was supported by a collaborative research grant (Grant 0137/88) from NATO, by the Danish Natural Science Research Council, and by the Ministero della Pubblica Istruzione of Italy. We thank Dr. K. B. Hansen, Dr. J. Fenger, and E. Engholm Larsen for continual support with the experimental facility. We also thank Dr. O. F. Nielsen at the Chemical Laboratory V, H. C. Ørsted Institute, University of Copenhagen, for help with the recording of ground-state Raman spectra.

Registry No. (*E*)-2,5-Dimethyl-1,3,5-hexatriene, 41233-74-3; (*Z*)-2,5-dimethyl-1,3,5-hexatriene, 49839-76-1; (*E*)-3,4-d_2-2,5-dimethyl-1,3,5-hexatriene, 117566-51-5; (*Z*)-3,4-d_2-2,5-dimethyl-1,3,5-hexatriene, 134879-35-9; (*E*)-3-*d*-2,5-dimethyl-1,3,5-hexatriene, 117566-50-4.

Supplementary Material Available: Computed wavenumbers, assignments, and Stokes shift parameters γ for the *tZt*, *tZc*, *cZc*, *tPt*, *cPc*, and *tPc* forms of DMHT and some of their duteriated derivatives (7 pages). Ordering information is given on any current masthead page.

(24) Arai, T.; Sakuragi, H.; Tokumaru, K.; Sakaguchi, Y.; Nakamura, J.; Hayashi, H. *Chem. Phys. Lett.* **1983**, *98*, 40.